Hairpin Peptide Motif. A New Class of Oligopeptides for Sequence-Specific Recognition in the Minor Groove of Double-Helical DNA

Milan Mrksich, Michelle E. Parks, and Peter B. Dervan*

Contribution from the Arnold and Mabel Beckman Laboratories of Chemical Synthesis, California Institute of Technology, Pasadena, California 91125

Received March 7, 1994[⊕]

Abstract: Peptides which bind in the minor groove of DNA as antiparallel side-by-side dimers can be linked head-to-tail to afford a new class of hairpin oligopeptides with enhanced sequence specificity for DNA. Four hexapeptides were synthesized wherein the terminal amine and carboxyl groups of tris(*N*-methylpyrrolecarboxamide) (P3) and *N*-methylimidazole-2-carboxamide–netropsin (2-ImN), respectively, have been connected with glycine (Gly), β-alanine (βAla), 4-aminobutyric acid (GABA), and 5-aminovaleric acid (Ava) amino acids. The hexapeptide 2-ImN-GABA-P3 binds 5'-TGTTA-3' sites with a binding affinity of 7.6×10^7 M^{-1} (10 mM Tris·HCl, 10 mM KCl, 10 mM MgCl$_2$, and 5 mM CaCl$_2$ at pH 7.0 and 22 °C). The general and efficient synthetic methodology for preparation of head-to-tail linked peptides should allow the design of a new class of hairpin peptides for specific recognition of many different sequences in the minor groove of DNA.

Recent 2:1 peptide–DNA complexes have created new models for the design of nonnatural ligands for sequence-specific recognition in the minor groove of DNA.[1-4] An imidazole-pyrrole–pyrrole tripeptide, 1-methylimidazole-2-carboxamide-netropsin (2-ImN), was shown to specifically bind the mixed sequence 5'-(A,T)G(A,T)C(A,T)-3' as a side-by-side antiparallel dimer.[2] In addition to the sequence-dependent minor groove width being a determinant of specificity, the 2:1 model allows specific contacts with *each strand* on the floor of the minor groove.[1-4] The side-by-side combination of one imidazole ring on one ligand and a pyrrolecarboxamide on the second ligand recognizes G·C, while a pyrrolecarboxamide/imidazole pair targets a C·G base pair.[2-4] A pyrrolecarboxamide/pyrrolecarboxamide combination is partially degenerate and binds to either A·T or T·A base pairs.[1-4]

For some DNA sequences, a single peptide will suffice, such as the case of the crescent-shaped 2-ImN which binds 5'-TGACA-3' as a homodimer.[2] However, when two *different* peptides bind a sequence as a *heterodimer*, there is the added complexity of each peptide having specific affinity for other sequences as well.[3,4] For example, the peptides 2-ImN and distamycin (D) bind the sequence 5'-TGTTA-3' as a heterodimer and simultaneously bind with comparable affinity the sites 5'-(A,T)$_5$-3' (by D) and 5'-TGACA-3' (by 2-ImN) as well (Figure 1).[3] For those cases where *different* peptides contact each strand of the minor groove, there is a need to design motifs that link the side-by-side peptides to favor the heterodimeric binding site.

We recently reported that peptides tethered through the central pyrrole rings with a butyl linker bind with increased affinity and specificity.[5,6] However, the synthetic methodology for preparation of this class of covalent peptide dimers may not be easily extended

(2-ImN / D) • TGTTA
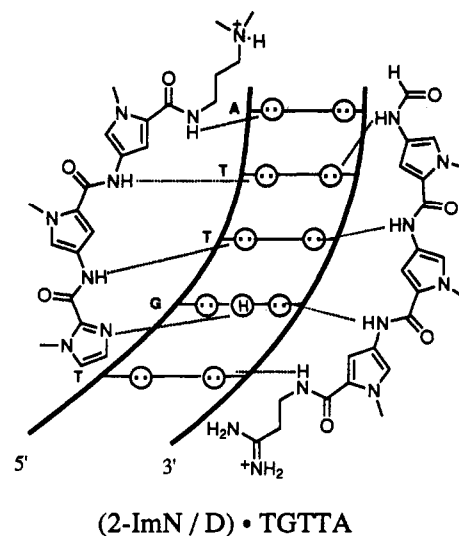
Figure 1. Heterodimeric binding model for the complex formed between 2-ImN and D and a 5'-TGTTA-3' sequence.[3] Circles with dots represent lone pairs of N3 of purines and O2 of pyrimidines. Circles containing an H represent the N2 hydrogen of guanine. Putative hydrogen bonds are illustrated by dotted lines.

to the synthesis of other peptide analogs. We report here a second-generation peptide motif which offers a more general synthetic methodology for the preparation of a wide variety of covalent peptide dimers.

Hairpin Peptide Motif. The design of the first-generation covalent peptide dimers was based on the proximity of the two *N*-methyl groups of the central pyrroles in the 2:1 complex. Alternatively, the two peptides could also be joined at their ends if a suitable "turn peptide" could be found which fits in the minor groove of DNA and does not perturb the side-by-side peptide–DNA complex geometry. Within the antiparallel 2-ImN/D·5'-TGTTA-3' complex, the terminal carboxyl group of 2-ImN and

⊕ Abstract published in *Advance ACS Abstracts,* August 15, 1994.

(1) (a) Pelton, J. G.; Wemmer, D. E. *Proc. Natl. Acad. Sci. U.S.A.* **1989,** *86,* 5723–5727. (b) Pelton, J. G.; Wemmer, D. E. *J. Am. Chem. Soc.* **1990,** *112,* 1393–1399. (c) Chen, X.; Ramakrishnan, B.; Rao, S. T.; Sundaralingam, M. *Struct. Biol. Nat.* **1994,** *1,* 169–175.

(2) (a) Wade, W. S.; Mrksich, M.; Dervan, P. B. *J. Am. Chem. Soc.* **1992,** *114,* 8783–8794. (b) Mrksich, M.; Wade, W. S.; Dwyer, T. J.; Geierstanger, B. H.; Wemmer, D. E.; Dervan, P. B. *Proc. Natl. Acad. Sci. U.S.A.* **1992,** *89,* 7586–7590. (c) Wade, W. S.; Mrksich, M.; Dervan, P. B. *Biochemistry* **1993,** *32,* 11385–11389.

(3) (a) Mrksich, M.; Dervan, P. B. *J. Am. Chem. Soc.* **1993,** *115,* 2572–2576. (b) Geierstanger, B. H.; Jacobsen, J-P.; Mrksich, M.; Dervan, P. B.; Wemmer, D. E. *Biochemistry* **1994,** *33,* 3055.

(4) Geierstanger, B. H.; Dwyer, T. J.; Bathini, Y.; Lown, J. W.; Wemmer, D. E. *J. Am. Chem. Soc.* **1993,** *115,* 4474–4482.

(5) For covalent homodimer peptides see: (a) Mrksich, M.; Dervan, P. B. *J. Am. Chem. Soc.* **1993,** *115,* 9892–9899. (b) Dwyer, T. J.; Geierstanger, B. H.; Mrksich, M.; Dervan, P. B.; Wemmer, D. E. *J. Am. Chem. Soc.* **1993,** *115,* 9900–9906.

(6) For covalent heterodimer peptides see: Mrksich, M.; Dervan, P. B. *J. Am. Chem. Soc.* **1994,** *116,* 3663–3664.
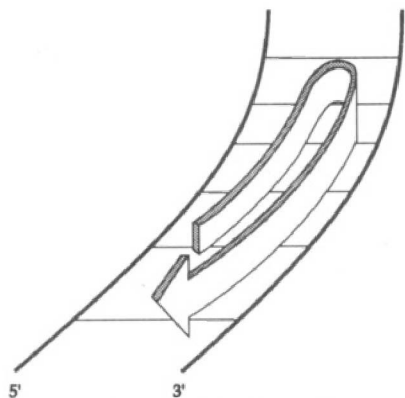
Figure 2. Model for binding of a hairpin peptide–turn–peptide in the minor groove of DNA.
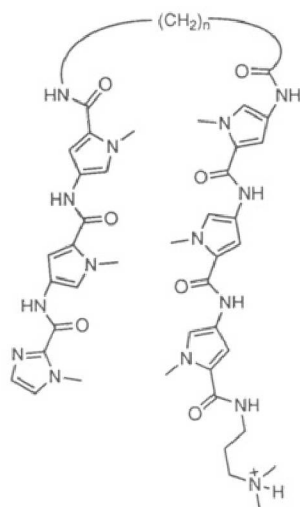
n = 1: 2-ImN-GLY-P3
n = 2: 2-ImN-βALA-P3
n = 3: 2-ImN-GABA-P3
n = 4: 2-ImN-AVA-P3

Figure 3. Hexapeptides 2-ImN-Gly-P3, 2-ImN-βAla-P3, 2-ImN-GABA-P3, and 2-ImN-Ava-P3 wherein the terminal carboxylic acid of 2-ImN and the terminal amine of P3 are connected with glycine, β-alanine, γ-aminobutyric acid, and 5-aminovaleric acid, respectively.

the terminal amine of tris(*N*-methylpyrrolecarboxamide) (P3) are positioned for linking with amino acids which allow the linear peptide "dimer" to *fold back* on itself (Figure 2). A series of peptides were synthesized wherein the C-terminal carboxylic acid of 2-ImN and the N-terminal amine of P3 were connected with simple amino acids which differ incrementally in length by one methylene unit; glycine (Gly), β-alanine (βAla), γ-aminobutyric acid (GABA), and 5-aminovaleric acid (Ava) (Figure 3). The binding affinities of the four hexapeptides 2-ImN-Gly-P3, 2-ImN-βAla-P3, 2-ImN-GABA-P3, and 2-ImN-Ava-P3 for three sites, 5'-TTTTT-3', 5'-TGTTA-3', and 5'-TGACA-3', on a 135 base pair DNA fragment were determined by quantitative DNase I footprint titration experiments.

Results

Synthesis of Hexapeptides. The peptides are synthesized in four steps from previously described intermediates (Figure 4). Reduction of the nitrotris(*N*-methylpyrrolecarboxamide)[7] (300 psi of H₂, Pd/C) and coupling with the *N*-(*tert*-butoxycarbonyl)-amino acid (DCC, HOBt) afforded peptides **2a–d**. Deprotection of the amine (TFA, CH₂Cl₂) and coupling with *N*-methyl-4-(*N*-methyl-4-nitropyrrole-2-carboxamido)pyrrole-2-carboxylic acid[8] (DCC, HOBt) yielded **4a–d** in 85% yield. Reduction of the

(7) Taylor, J. S.; Schultz, P. G.; Dervan, P. B. *Tetrahedron* **1984**, *40*, 457.

nitropyrrole (300 psi of H₂, Pd/C) and coupling to 1-methylimidazole-2-carboxylic acid (DCC, HOBt) provided the hexapeptides 2-ImN-Gly-P3, 2-ImN-βAla-P3, 2-ImN-GABA-P3 and 2-ImN-Ava-P3. The solubility of the four peptides has a strong even–odd dependence on the linker length. 2-ImN-Gly-P3 and 2-ImN-GABA-P3 were freely soluble in aqueous solution. 2-ImN-βAla-P3 and 2-ImN-Ava-P3 were soluble only at concentrations of less than 1.0 mM.

Footprinting. DNase I footprinting[9] on the 3'-³²P-end-labeled 135 base pair *Eco*RI/*Bsr*BI restriction fragment (10 mM Tris·HCl, 10 mM KCl, 10 mM MgCl₂, and 5 mM CaCl₂ at pH 7.0 and 22 °C) reveal that two peptides, 2-ImN-Gly-P3 and 2-ImN-GABA-P3, specifically bind the five base pair sites in the relative order 5'-TGTTA-3' > 5'-TGACA-3' > 5'-TTTTT-3'. Two peptides, 2-ImN-βAla-P3 and 2-ImN-Ava-P3, bound all sites with weak affinity. The apparent first-order binding affinities of the four peptides for the three sites were determined by quantitative DNase I footprint titration experiments (Table 1). 2-ImN-GABA-P3 binds the 5'-TGTTA-3' site with the highest affinity, 7.6×10^7 M⁻¹. Moreover, this peptide binds the single "mismatched" site TGACA with a lower affinity of 3.2×10^6 M⁻¹, displaying the best specificity between these two sites. The θ_{app} points for 2-ImN-Gly-P3 binding the 5'-TGTTA-3' and 5'-TGACA-3' sites are steeper than expected for a 1:1 complex of peptide with DNA. The data points are adequately fit by a cooperative binding isotherm consistent with intermolecular dimeric binding.[1c] The data for 2-ImN-GABA-P3 binding these sites were best fit with a Langmuir binding isotherm consistent with a 1:1 complex of peptide with DNA. For all peptides binding the 5'-TTTTT-3' site, the binding affinities were less than 5×10^5 M⁻¹ and are approximate since the quality of fits and the standard deviations for these data sets were poor.

Discussion

Binding Affinities. Among the four hexapeptides, 2-ImN-GABA-P3 binds the 5'-TGTTA-3' site with the highest affinity ($\sim 10^8$ M⁻¹) and sequence specificity which suggests that the hexapeptide binds this site as an intramolecular hairpin structure (Figure 8). Importantly, the peptide binds the mismatched 5'-TGACA-3' site with 24-fold lower affinity. Linking the peptides through the terminal amine and carboxylic acid groups is an effective strategy for improving the sequence *specificities* of different antiparallel side-by-side peptides for DNA sites. We estimate that the increase in affinity of these hairpin linked peptides over the uncoupled components is at least 2 orders of magnitude. This modest energetic gain is not unreasonable when one considers the decrease in the number of positive charges in the DNA–ligand complex in proceeding from the antiparallel dimer motif (two charges) to the hairpin motif (one charge) should be energetically unfavorable. In addition, restricting rotational freedom of the three methylene units in the GABA linker as a loop in the minor groove must have some entropic penalty.

A comparison of the binding affinities of the four peptides for the 5'-TGTTA-3' site reveals that the linker length has a dramatic effect on overall complex stability. Modeling suggested that glycine and β-alanine linkers would not favorably accommodate binding of 2-ImN-Gly-P3 and 2-ImN-βAla-P3 in the minor groove of DNA as hairpin peptides. Consistent with the cooperative binding isotherms from the quantitative footprint titration experiments, 2-ImN-Gly-P3 peptide likely binds as an intermolecular dimer. Moreover, this peptide displays a larger binding

(8) (a) Bialer, M.; Yagen, B.; Mechoulam, R. *Tetrahedron* **1978**, *34*, 2389–2391. (b) Lown, J. W.; Krowicki, K. *J. Org. Chem.* **1985**, *50*, 3774–3779.
(9) (a) Galas, D.; Schmitz, A. *Nucleic Acids Res.* **1978**, *5*, 3157–3170. (b) Fox, K. R.; Waring, M. *J. Nucleic Acids Res.* **1984**, *12*, 9271–9285.
(10) (a) Brenowitz, M.; Senear, D. F.; Shea, M. A.; Ackers, G. K. *Methods Enzymol.* **1986**, *130*, 132–181. (b) Brenowitz, M.; Senear, D. F.; Shea, M. A.; Ackers, G. K. *Proc. Natl. Acad. Sci. U.S.A.* **1986**, *83*, 8462–8466. (c) Senear, D. F.; Brenowitz, M.; Shea, M. A.; Ackers, G. K. *Biochemistry* **1986**, *25*, 7344–7354.
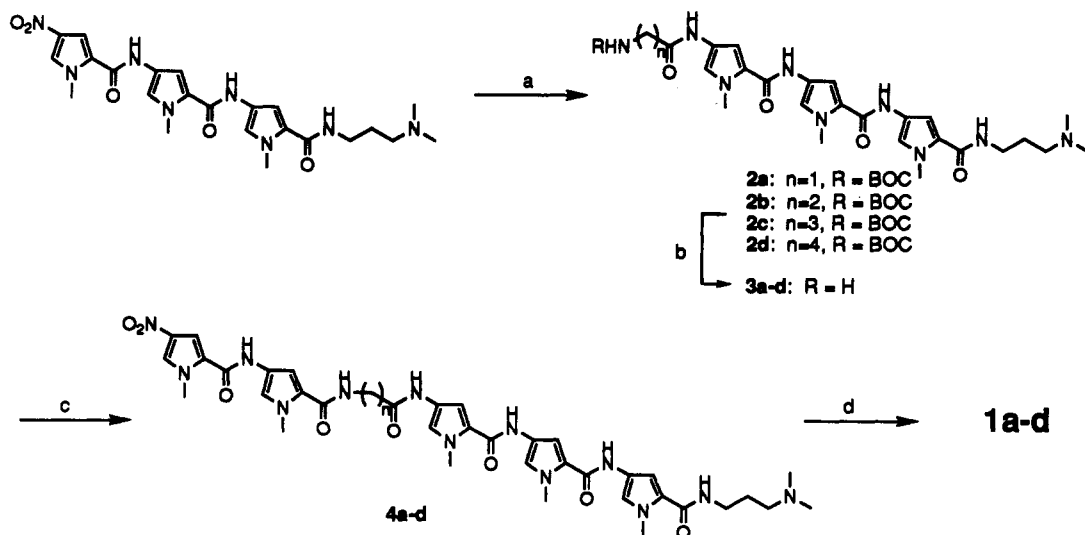
Figure 4. Synthetic scheme for 2-ImN-Gly-P3, 2-ImN-βAla-P3, 2-ImN-GABA-P3, and 2-ImN-Ava-P3: (a) (i) 300 psi of H_2, 10% Pd/C; (ii) BocNH(CH$_2$)$_n$CO$_2$H, DCC, HOBt; (b) TFA/CH$_2$Cl$_2$; (c) (i) 300 psi of H_2, 10% Pd/C; (ii) N-methyl-4-(N-methyl-4-nitropyrrole-2-carboxamido)-pyrrole-2-carboxylic acid, DCC, HOBt; (d) (i) 300 psi of H_2, 10% Pd/C; (ii) 1-methylimidazole-2-carboxylic acid, DCC, HOBt.
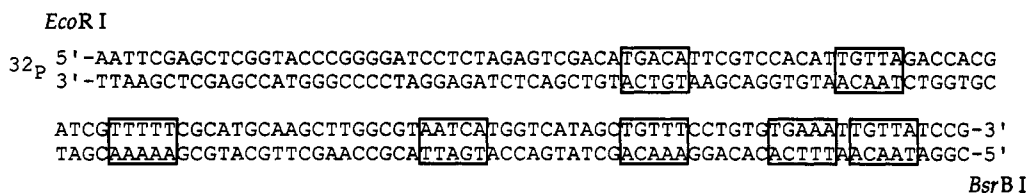
Figure 5. Sequence of the 135 base pair *Eco*RI/*Bsr*BI restriction fragment. Three five base pair sites, 5′-TTTTT-3′, 5′-TGTTA-3′, and 5′-TGACA-3′, proximal to the ^{32}P label at the *Eco*RI site were analyzed by quantitative footprint titration analysis. Note that there are additional binding sites on the upper half of the autoradiogram (Figure 6) of sequence composition (A,T)G(A,T)$_3$ which are also occupied by 2-ImN-GABA-P3.

site size (data not shown) which may result from binding in the minor groove by extended conformations of two peptides, creating a larger nonspecific steric blockade adjacent to the 5′-TGTTA-3′ site to cleavage by DNase I. We defer further speculation about these complexes until structural data from NMR spectroscopy are available.

Implications for the Design of Minor-Groove-Binding Molecules. We anticipate that the general and efficient synthetic methodology for preparation of GABA-linked peptides will allow the design of a new class of hairpin peptides for specific recognition of many different sequences. This strategy involves the construction of a peptide subunit for recognition in the minor groove of DNA of one strand of the binding site, the GABA linker for the turn, and a second peptide subunit for recognition of the other strand. The next generation of hairpin peptides should implement a linker which enforces a turn and disfavors binding of the peptide in extended conformations which allow 1:1 or intermolecular 2:1 complexes by the tripeptide subunits. Formally, this can be accomplished by either introducing rigid amino acid linkers or, alternatively, preparing cyclic peptides incorporating two GABA linkers.

Experimental Section

^{1}H NMR and ^{13}C NMR spectra were recorded on a General Electric-QE 300 NMR spectrometer in CD$_3$OD or DMSO-d_6, with chemical shifts reported in parts per million relative to residual CHD$_2$OD or DMSO-d_5, respectively. The ^{13}C resonances for pyrrole methyl groups are overlapped by resonances from the solvent and in general are not listed. IR spectra were recorded on a Perkin-Elmer FTIR spectrometer. High-resolution mass spectra were recorded using fast atom bombardment (FABMS) techniques at the Mass Spectrometry Laboratory at the University of California, Riverside. Reactions were executed under an inert argon atmosphere. Reagent grade chemicals were used as received unless otherwise noted. Tetrahydrofuran (THF) was distilled under nitrogen from sodium/benzophenone ketyl. Dichloromethane (CH$_2$Cl$_2$) and triethylamine were distilled under nitrogen from powdered calcium

hydride. Dimethylformamide (DMF) was purchased as an anhydrous solvent from Aldrich. Flash chromatography was carried out using EM Science Kieselgel 60 (230–400) mesh.[11] Thin-layer chromatography was performed on EM Reagents silica gel plates (0.5 mm thickness). All compounds were visualized with short-wave ultraviolet light.

N-(tert-Butoxycarbonyl)amino Acid–Tris(*N*-methylpyrrolecarboxamide)s 2a–d (Exemplified with 2a). To a solution of *N*-(*tert*-butoxy-carbonyl)glycine (780 mg, 4.46 mmol) in dimethylformamide (4.0 mL) was added a solution of dicyclohexylcarbodiimide (464 mg, 2.25 mmol) in methylene chloride (4.5 mL), and the solution was stirred for 30 min. Separately, a solution of tris(*N*-methylpyrrolecarboxamide) (300 mg, 0.60 mmol) and palladium on carbon (10%, 100 mg) in dimethylformamide (9.0 mL) was stirred under a hydrogen atmosphere (300 psi) in a Parr bomb apparatus for 3 h. The reaction mixture was filtered through Celite to remove catalyst, and the filtrate was added to the activated acid, followed by stirring for 2 h. The mixture was filtered through Celite, solvents were removed *in vacuo*, and the residue was purified by flash column chromatography (0.5% ammonium hydroxide in methanol) to afford 2a.

Data for 2a: yield 86% (331 mg); ^{1}H NMR (CD$_3$OD) δ 7.18 (d, 1 H, *J* = 1.9 Hz), 7.16 (d, 1 H, *J* = 1.9 Hz), 7.14 (d, 1 H, *J* = 1.8 Hz), 6.91 (d, 1 H, *J* = 1.9 Hz), 6.82 (d, 1 H, *J* = 1.9 Hz), 6.78 (d, 1 H, *J* = 1.9 Hz), 3.95 (bs, 2 H), 3.89 (s, 3 H), 3.88 (s, 3 H), 3.86 (s, 3 H), 3.29 (m, 2 H), 2.37 (t, 2 H, *J* = 7.4 Hz), 2.23 (s, 6 H), 1.73 (m, 2 H), 1.43 (s, 9 H); ^{13}C NMR (CD$_3$OD) δ 169.5, 164.1, 161.2, 161.1, 158.4, 124.5, 123.2, 122.7, 120.7, 120.6, 120.4, 106.4, 106.1, 106.0, 80.7, 58.2, 44.9, 44.6, 38.5, 36.8, 28.7, 28.2; IR (thin film) 3300 (m), 2942 (w), 1643 (s), 1581 (m), 1538 (s), 1464 (m), 1435 (m), 1405 (m), 1258 (m), 1208 (w), 1164 (m), 1106 (w), 775 (w) cm^{-1}; FABMS *m/e* 626.3415 (M + H, 626.3432 calcd for C$_{31}$H$_{46}$N$_9$O$_6$).

Data for 2b: yield 83% (320 mg); ^{1}H NMR (CD$_3$OD) δ 7.15 (d, 1 H, *J* = 1.8 Hz), 7.13 (d, 1 H, *J* = 1.8 Hz), 7.07 (d, 1 H, *J* = 1.8 Hz), 6.89 (d, 1 H, *J* = 1.9 Hz), 6.83 (d, 1 H, *J* = 1.7 Hz), 6.78 (d, 1 H, *J* = 1.9 Hz), 3.85 (s, 3 H), 3.84 (s, 3 H), 3.82 (s, 3 H), 3.30 (m, 4 H), 2.49 (t, 2 H, *J* = 6.8 Hz), 2.41 (t, 2 H, *J* = 7.4 Hz), 2.27 (s, 6 H), 1.77 (m, 2 H), 1.42 (s, 9 H); ^{13}C NMR (CD$_3$OD) δ 170.9, 164.1, 161.3, 158.3, 124.6, 124.5, 123.3, 123.2, 120.8, 120.6, 120.4, 106.5, 106.0, 105.8, 80.1,

(11) Still, W. C.; Kahn, M.; Mitra, A. *J. Org. Chem.* **1978**, *40*, 2923–2925.
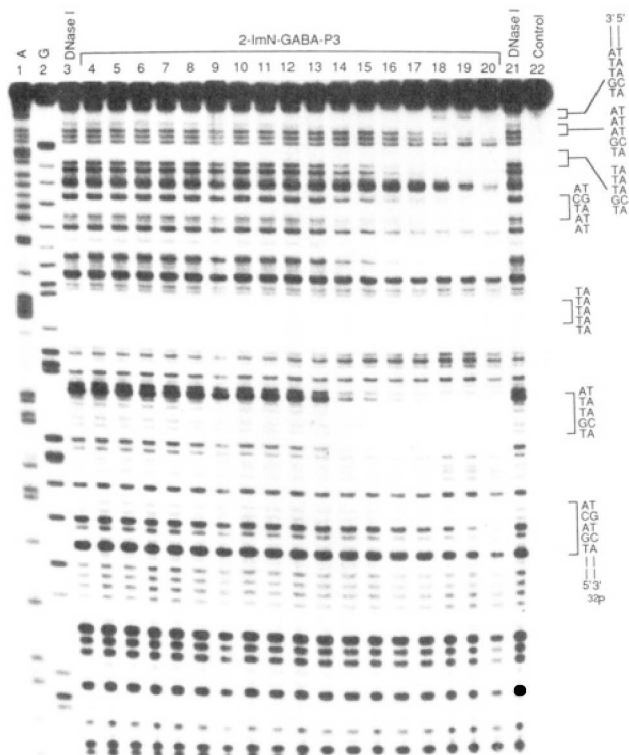
Figure 6. Quantitative DNase I footprint titration experiment with 2-ImN-GABA-P3 on the 3′-³²P-labeled 135 base pair *Eco*RI/*Bsr*BI restriction fragment from plasmid pMM5: lane 1, A reaction; lane 2, G reaction; lanes 3 and 21, DNase I standard; lanes 4–20, 10 pM, 20 pM, 50 pM, 100 pM, 200 pM, 500 pM, 1 nM, 2 nM, 5 nM, 10 nM, 20 nM, 50 nM, 100 nM, 200 nM, 500 nM, 1 μM, and 2 μM 2-ImN-GABA-P3, respectively; lane 22, intact DNA. The 5′-TTTTT-3′, 5′-TGTTA-3′, and 5′-TGACA-3′ binding sites which were analyzed are shown on the right side of the autoradiogram. Additional sites not analyzed are 5′-AATCA-3′, 5′-TGTTT-3′, 5′-TGAAA-3′, and 5′-TGTTA-3′. All reactions contain a 20 kcpm restriction fragment, 10 mM Tris·HCl, 10 mM KCl, 10 mM MgCl₂, and 5 mM CaCl₂.
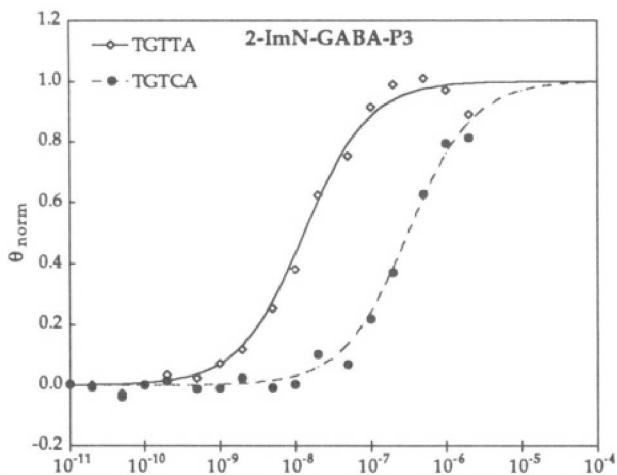
Figure 7. Data for the quantitative DNase I footprint titration experiments for 2-ImN-GABA-P3 in complex with the 5′-TGTTA-3′ (match) and 5′-TGACA-3′ (single mismatch) sites. The θ_{norm} points were obtained using photostimulable storage phosphor autoradiography and processed as described in the Experimental Section. The data points for the 5′-TGTTA-3′ site are indicated by open diamonds and for the 5′-TGACA-3′ site by filled circles. The solid and dashed curves are the best fit Langmuir binding titration isotherms obtained from a nonlinear least-squares algorithm using eq 2.

58.3, 45.4, 38.6, 38.0, 37.5, 36.8, 36.7, 28.7, 28.3; IR (thin film) 3293 (m), 2944 (w), 1637 (s), 1578 (m), 1542 (m), 1459 (s), 1406 (m), 1260 (m), 1208 (w), 1161 (m), 775 (w) cm⁻¹; FABMS *m/e* 640.3571 (M + H, 640.3573 calcd for $C_{30}H_{44}N_9O_6$).
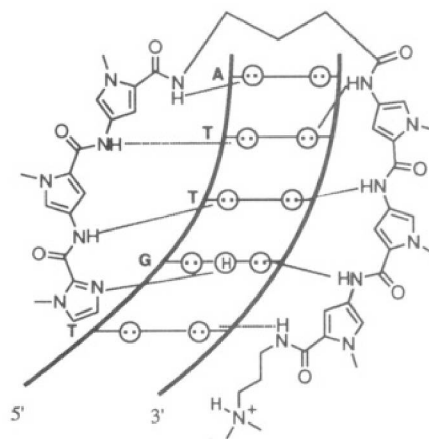
2-ImN-GABA-P3 • TGTTA

Figure 8. Model for the complex formed between the hexapeptide 2-ImN-GABA-P3 and the 5′-TGTTA-3′ site. Circles with dots represent lone pairs of N3 of purines and O2 of pyrimidines. Circles containing an H represent the N2 hydrogen of guanine. Putative hydrogen bonds are illustrated by dotted lines.

Table 1. Apparent First-Order Binding Constants $(M^{-1})^{a,b}$

peptide	binding site		
	5′-TTTTT-3′ ^{c}	5′-TGTTA-3′	5′-TGACA-3′
2-ImN-Gly-P3	$<5 \times 10^5$	2.2×10^7 (0.2)	$\leq 6 \times 10^6$
2-ImN-βAla-P3	$<5 \times 10^5$	$\leq 2 \times 10^6$	$<5 \times 10^5$
2-ImN-GABA-P3	$<5 \times 10^5$	7.6×10^7 (0.8)	3.2×10^6 (0.7)
2-ImN-Ava-P3	$<5 \times 10^5$	$<5 \times 10^5$	$<5 \times 10^5$

^{a} Values reported are the mean values measured from three footprint titration experiments, with the standard deviation for each data set indicated in parentheses. ^{b} The assays were performed at 22 °C at pH 7.0 in the presence of 10 mM Tris·HCl, 10 mM KCl, 10 mM MgCl₂, and 5 mM CaCl₂. ^{c} Approximate binding affinities are reported since the quality of fits and standard deviations for these data sets were poor.

Data for 2c: yield 79% (70 mg); ¹H NMR (CD₃OD) δ 7.16 (d, 1 H, *J* = 1.9 Hz), 7.14 (d, 1 H, *J* = 1.9 Hz), 7.12 (d, 1 H, *J* = 1.6 Hz), 6.90 (d, 1 H, *J* = 1.7 Hz), 6.81 (d, 1 H, *J* = 1.6 Hz), 6.77 (d, 1 H, *J* = 1.7 Hz), 3.87 (s, 3 H), 3.86 (s, 3 H), 3.84 (s, 3 H), 3.30 (m, 2 H), 3.08 (t, 2 H, *J* = 6.9 Hz), 2.38 (t, 2 H, *J* = 7.8 Hz), 2.32 (t, 2 H, *J* = 7.5 Hz), 2.24 (s, 6 H), 1.77 (m, 4 H), 1.41 (s, 9 H); ¹³C NMR (CD₃OD) δ 170.7, 162.2, 159.4, 156.5, 122.6, 122.5, 121.2, 118.8, 118.6, 118.4, 104.5, 104.0, 103.9, 78.0, 56.3, 43.4, 38.9, 34.8, 26.8, 26.3, 25.4; IR (thin film) 3301 (m), 2938 (w), 1638 (s), 1578 (m), 1534 (s), 1461 (s), 1436 (s), 1405 (m), 1257 (m), 1205 (w), 1164 (m) cm⁻¹; FABMS *m/e* 654.3728 (M + H, 654.3695 calcd for $C_{32}H_{48}N_9O_6$).

Data for 2d: yield 84% (385 mg); ¹H NMR (CD₃OD) δ 7.17 (d, 1 H, *J* = 1.9 Hz), 7.16 (d, 1 H, *J* = 1.9 Hz), 7.13 (d, 1 H, *J* = 1.9 Hz), 6.91 (d, 1 H, *J* = 1.9 Hz), 6.82 (d, 1 H, *J* = 1.9 Hz), 6.78 (d, 1 H, *J* = 1.9 Hz), 3.89 (s, 3 H), 3.87 (s, 3 H), 3.85 (s, 3 H), 3.30 (m, 2 H), 3.05 (t, 2 H, *J* = 6.8 Hz), 2.41 (t, 2 H, *J* = 7.6 Hz), 2.32 (t, 2 H *J* = 7.4 Hz), 2.26 (s, 6 H), 1.76 (m, 2 H), 1.68 (m, 2 H), 1.51 (m, 2 H), 1.42 (s, 9 H); ¹³C NMR (CD₃OD) δ 173.1, 164.1, 161.3, 158.5, 124.6, 124.5, 123.2, 120.8, 120.6, 120.4, 106.5, 106.0, 105.9, 79.8, 58.3, 45.4, 40.9, 38.6, 36.8, 30.5, 28.8, 28.3, 24.3; IR (thin film) 3298 (m), 2941 (w), 1642 (s), 1580 (m), 1536 (s), 1466 (m), 1435 (m), 1406 (m), 1258 (m), 1208 (w), 1168 (m), 776 (w) cm⁻¹; FABMS *m/e* 668.3884 (M + H, 668.3865 calcd for $C_{33}H_{50}N_9O_6$).

Amino Acid–Tris(*N*-methylpyrrolecarboxamide)s 3a–d (Exemplified with 3b). To a solution of protected amine **2b** (335 mg, 0.535 mmol) in methylene chloride (13.0 mL) was added trifluoroacetic acid (3.0 mL), and the resulting solution was stirred for 20 min. Hexanes (200 mL) were added, and the solution was stirred for 10 min during which an oil separated. The solvent was removed by decantation, the residue was dissolved in 6% NH₄OH/MeOH (100 mL), and the solvent was removed *in vacuo*. Purification of the oil by flash column chromatography (8% ammonium hydroxide in methanol) afforded amine **3b**.

Data for 3a: yield 99% (256 mg); ¹H NMR (CD₃OD) δ 7.15 (d, 1 H, *J* = 1.8 Hz), 7.14 (d, 1 H, *J* = 1.8 Hz), 7.13 (d, 1 H, *J* = 1.9 Hz), 6.90 (d, 1 H, *J* = 1.8 Hz), 6.83 (d, 1 H, *J* = 1.8 Hz), 6.77 (d, 1 H, *J* = 1.8

Hz), 3.86 (s, 3 H), 3.85 (s, 3 H), 3.83 (s, 3 H), 3.37 (s, 2 H), 3.30 (m, 2 H), 2.41 (t, 2 H, *J* = 7.7 Hz), 2.27 (s, 6 H), 1.75 (m, 2 H); ^{13}C NMR (CD$_3$OD) δ 171.3, 163.3, 160.5, 160.4, 123.8, 122.4, 122.3, 120.0, 119.7, 119.6, 105.6, 105.2, 105.0, 57.4, 48.2, 44.5, 44.3, 37.7, 36.0, 27.3; IR (thin film) 3300 (s), 1638 (s), 1578 (s), 1546 (s), 1438 (m), 1406 (m), 1262 (w), 1208 (w), 1149 (w), 1108 (w) cm^{-1}; FABMS *m/e* 526.2912 (M + H, 526.2890 calcd for C$_{25}$H$_{36}$N$_9$O$_4$).

Data for 3b: yield 91% (264 mg); ^{1}H NMR (CD$_3$OD) δ 7.16 (d, 1 H, *J* = 1.9 Hz), 7.15 (d, 1 H, *J* = 1.9 Hz), 7.14 (d, 1 H, *J* = 1.9 Hz), 6.91 (d, 1 H, *J* = 1.9 Hz), 6.82 (d, 1 H, *J* = 1.9 Hz), 6.77 (d, 1 H, *J* = 1.9 Hz), 3.88 (s, 3 H), 3.87 (s, 3 H), 3.85 (s, 3 H), 3.30 (m, 2 H), 2.95 (t, 2 H, *J* = 6.6 Hz), 2.48 (t, 2 H, *J* = 6.6 Hz), 2.38 (t, 2 H, *J* = 7.6 Hz), 2.25 (s, 6 H), 1.75 (m, 2 H); ^{13}C NMR (CD$_3$OD) δ 170.6, 163.3, 160.5, 160.4, 123.8, 123.7, 122.4, 122.3, 120.0, 119.7, 119.5, 105.6, 105.2, 105.0, 57.5, 47.3, 44.6, 38.6, 38.1, 37.8, 35.9, 27.4; IR (thin film) 3336 (s), 1638 (s), 1578 (s), 1560 (s), 1540 (s), 1466 (m), 1458 (m), 1406 (m), 1263 (w), 1209 (w), 1151 (w), 1108 (w) cm^{-1}; FABMS *m/e* 540.3047 (M + H, 540.3051 calcd for C$_{26}$H$_{38}$N$_9$O$_4$).

Data for 3c: yield 91% (54 mg); ^{1}H NMR (CD$_3$OD) δ 7.17 (d, 1 H, *J* = 1.9 Hz), 7.16 (d, 1 H, *J* = 1.9 Hz), 7.13 (d, 1 H, *J* = 1.9 Hz), 6.91 (d, 1 H, *J* = 1.8 Hz), 6.82 (d, 1 H, *J* = 1.8 Hz), 6.77 (d, 1 H, *J* = 1.9 Hz), 3.88 (s, 3 H), 3.87 (s, 3 H), 3.85 (s, 3 H), 3.30 (m, 2 H), 2.67 (t, 2 H, *J* = 7.3 Hz), 2.41–2.32 (m, 4 H), 2.24 (s, 6 H), 1.20 (m, 4 H); ^{13}C NMR (CD$_3$OD) δ 170.5, 163.3, 160.4, 160.3, 123.8, 123.7, 121.1, 120.0, 119.7, 119.5, 105.7, 105.2, 105.0, 57.5, 44.6, 41.2, 37.8, 38.1, 36.0, 35.9, 33.8, 29.2, 27.4; IR (thin film) 3286 (s), 1637 (s), 1580 (s), 1560 (s), 1538 (s), 1466 (m), 1436 (s), 1406 (m), 1262 (w), 1209 (w), 1156 (w), 1108 (w) cm^{-1}; FABMS *m/e* 554.3203 (M + H, 554.3207 calcd for C$_{27}$H$_{40}$N$_9$O$_4$).

Data for 3d: yield 96% (312 mg); ^{1}H NMR (CD$_3$OD) δ 7.17 (d, 1 H, *J* = 1.9 Hz), 7.16 (d, 1 H, *J* = 1.9 Hz), 7.14 (d, 1 H, *J* = 1.9 Hz), 6.92 (d, 1 H, *J* = 1.9 Hz), 6.83 (d, 1 H, *J* = 1.9 Hz), 6.78 (d, 1 H, *J* = 1.9 Hz), 3.87 (s, 3 H), 3.85 (s, 3 H), 3.83 (s, 3 H), 3.30 (m, 2 H), 3.86 (t, 2 H, *J* = 7.2 Hz), 2.37 (t, 2 H, *J* = 7.6 Hz), 2.32 (t, 2 H, *J* = 7.3 Hz), 2.23 (s, 6 H), 1.72 (m, 4 H), 1.53 (m, 2 H); ^{13}C NMR (CD$_3$OD) δ 172.9, 164.1, 161.3, 124.6, 124.5, 123.3, 120.8, 120.6, 120.4, 106.5, 106.0, 105.9, 58.3, 45.4, 41.7, 38.6, 36.8, 36.7, 32.2, 28.3, 24.4, 24.1; IR (thin film) 3287 (s), 2944 (w), 1644 (s), 1581 (s), 1556 (s), 1538 (s), 1467 (m), 1434 (s), 1406 (m), 1262 (m), 1209 (w), 1160 (w), 1107 (w) cm^{-1}; FABMS *m/e* 568.3360 (M + H, 568.3361 calcd for C$_{28}$H$_{42}$N$_9$O$_4$).

Nitrobis(*N*-methylpyrrolecarboxamide)–Amino Acid–Tris(*N*-methylpyrrolecarboxamide)s 4a–d (Exemplified with 4b). To a solution of bis(pyrrolecarboxylic acid) (303 mg, 1.04 mmol) and *N*-hydroxybenzotriazole hydrate (141 mg, 1.05 mmol) in dimethylformamide (2.1 mL) was added a solution of dicyclohexylcarbodiimide (217 mg, 1.05 mmol) in methylene chloride (2.1 mL), and the solution was stirred for 30 min. A solution of primary amine 3b (242 mg, 0.449 mmol) in dimethylformamide (3.0 mL) was added, and the mixture was stirred for 8 h. Methanol (1 mL) was added, and the reaction was filtered through Celite. The filtrate was concentrated *in vacuo* and purified by flash column chromatography (1% ammonium hydroxide in methanol) to afford 4b.

Data for 4a: yield 86% (323 mg); ^{1}H NMR (DMSO-*d$_6$*) δ 10.29 (s, 1 H), 9.92 (bs, 2 H), 9.89 (bs, 1 H), 8.37 (t, 1 H, *J* = 5.8 Hz), 8.18 (d, 1 H, *J* = 1.6 Hz), 8.07 (t, 1 H, *J* = 6.1 Hz), 7.59 (d, 1 H, *J* = 1.9 Hz), 7.27 (d, 1 H, *J* = 1.8 Hz), 7.23 (d, 1 H, *J* = 1.8 Hz), 7.18 (d, 1 H, *J* = 1.9 Hz), 7.17 (d, 1 H, *J* = 1.9 Hz), 7.02 (d, 1 H, *J* = 1.8 Hz), 6.94 (d, 1 H, *J* = 1.9 Hz), 6.92 (d, 1 H, *J* = 1.9 Hz), 6.81 (d, 1 H, *J* = 1.8 Hz), 3.95 (s, 3 H), 3.90 (bs, 2 H), 3.83 (s, 6 H), 3.82 (s, 3 H), 3.78 (s, 3 H), 3.34 (m, 2 H), 2.22 (t, 2 H, *J* = 7.1 Hz), 2.12 (s, 6 H), 1.59 (m, 2 H); IR (KBr) 3310 (m), 2934 (w), 1638 (s), 1578 (s), 1534 (s), 1466 (m), 1438 (s), 1406 (m), 1311 (s), 1256 (m), 1208 (m), 1107 (m) cm^{-1}; FABMS *m/e* 800.3592 (M + H, 800.3578 calcd for C$_{37}$H$_{46}$N$_{13}$O$_8$).

Data for 4b: yield 87% (319 mg); ^{1}H NMR (CD$_3$OD) δ 7.73 (d, 1 H, *J* = 1.8 Hz), 7.32 (d, 1 H, *J* = 1.9 Hz), 7.13 (d, 1 H, *J* = 1.8 Hz), 7.12 (d, 1 H, *J* = 1.9 Hz), 7.11 (d, 1 H, *J* = 1.9 Hz), 7.10 (d, 1 H, *J* = 1.9 Hz), 6.85 (d, 1 H, *J* = 1.9 Hz), 6.79 (d, 1 H, *J* = 1.9 Hz), 6.76 (d, 1 H, *J* = 1.9 Hz), 6.75 (d, 1 H, *J* = 1.9 Hz), 3.89 (s, 3 H), 3.82 (s, 3 H), 3.81 (s, 6 H), 3.79 (s, 3 H), 3.60 (bs, 2 H), 3.35 (m, 2 H), 2.58 (t, 2 H, *J* = 6.4 Hz), 2.35 (t, 2 H, *J* = 7.7 Hz), 2.22 (s, 6 H), 1.73 (m, 2 H); ^{13}C NMR (CD$_3$OD) δ 171.0, 164.1, 164.0, 161.3, 161.2, 159.5, 136.0, 128.6, 127.6, 124.6, 124.5, 123.1, 122.8, 120.8, 120.7, 120.5, 120.4, 108.7, 106.4, 106.0, 105.9, 58.3, 45.4, 38.6, 38.0, 37.1, 37.0, 36.8, 36.7, 28.3; IR (neat) 3284 (m), 2942 (w), 1638 (s), 1578 (s), 1534 (s), 1466 (m), 1438 (s), 1402 (m), 1308 (s), 1259 (m), 1207 (m), 1109 (w) cm^{-1}; FABMS *m/e* 814.3749 (M + H, 814.3739 calcd for C$_{38}$H$_{48}$N$_{13}$O$_8$).

Data for 4c: yield 81% (28 mg); ^{1}H NMR (CD$_3$OD) δ 7.78 (d, 1 H, *J* = 1.8 Hz), 7.35 (d, 1 H, *J* = 1.9 Hz), 7.15 (d, 1 H, *J* = 1.9 Hz), 7.14 (d, 1 H, *J* = 1.9 Hz), 7.13 (d, 1 H, *J* = 1.8 Hz), 7.06 (d, 1 H, *J* = 1.9 Hz), 6.86 (d, 1 H, *J* = 1.9 Hz), 6.79 (d, 2 H, *J* = 1.8 Hz), 6.76 (d, 1 H, *J* = 1.9 Hz), 3.94 (s, 3 H), 3.85 (s, 3 H), 3.84 (s, 3 H), 3.83 (s, 3 H), 3.81 (s, 3 H), 3.35 (q, 2 H, *J* = 5.6 Hz), 3.30 (m, 2 H), 2.38 (t, 2 H, *J* = 7.6 Hz), 2.24 (s, 6 H), 1.94 (m, 2 H), 1.75 (m, 2 H); ^{13}C NMR (CD$_3$OD) δ 172.8, 164.2, 161.3, 161.2, 159.5, 136.1, 128.7, 127.7, 124.6, 124.5, 124.4, 123.2, 123.1, 122.8, 120.8, 120.6, 120.4, 108.7, 106.4, 106.0, 58.4, 45.4, 39.9, 38.6, 38.1, 36.8, 34.9, 28.3, 27.0; IR (neat) 3281 (m), 2931 (w), 1633 (s), 1578 (m), 1530 (s), 1463 (m), 1434 (s), 1400 (s), 1308 (s), 1255 (m), 1205 (m), 1105 (w) cm^{-1}; FABMS *m/e* 828.3905 (M + H, 828.3923 calcd for C$_{39}$H$_{50}$N$_{13}$O$_8$).

Data for 4d: yield 87% (205 mg); ^{1}H NMR (CD$_3$OD) δ 7.76 (d, 1 H, *J* = 1.9 Hz), 7.35 (d, 1 H, *J* = 1.9 Hz), 7.14 (d, 1 H, *J* = 1.9 Hz), 7.13 (d, 2 H, *J* = 1.8 Hz), 7.09 (d, 1 H, *J* = 1.8 Hz), 6.87 (d, 1 H, *J* = 1.8 Hz), 6.81 (d, 1 H, *J* = 1.8 Hz), 6.79 (d, 1 H, *J* = 1.9 Hz), 6.75 (d, 1 H, *J* = 1.9 Hz), 3.92 (s, 3 H), 3.84 (s, 3 H), 3.83 (s, 3 H), 3.82 (s, 3 H), 3.81 (s, 3 H), 3.30 (m, 4 H), 2.34 (m, 4 H), 2.22 (s, 6 H), 1.72 (m, 4 H), 1.60 (m, 2 H); ^{13}C NMR (CD$_3$OD) δ 173.0, 164.1, 161.3, 159.5, 136.1, 128.7, 127.6, 124.8, 124.6, 124.5, 123.2, 122.8, 120.8, 120.6, 120.4, 108.7, 106.5, 106.0, 105.9, 105.8, 58.3, 45.4, 39.8, 38.6, 38.1, 36.8, 30.3, 28.3, 24.4; IR (neat) 3277 (m), 2942 (w), 1638 (s), 1578 (m), 1535 (s), 1460 (m), 1432 (s), 1401 (m), 1308 (m), 1258 (m), 1206 (m), 1109 (w) cm^{-1}; FABMS *m/e* 842.4062 (M + H, 842.4052 calcd for C$_{40}$H$_{52}$N$_{13}$O$_8$).

2-ImN–Amino Acid–P3 1a–d (Exemplified with 1d). To a solution of 1-methylimidazole-2-carboxylic acid (67 mg, 0.603 mmol) and *N*-hydroxybenzotriazole hydrate (82 mg, 0.60 mmol) in dimethylformamide (1.2 mL) was added a solution of 1,3-dicyclohexylcarbodiimide (124 mg, 0.60 mmol) in methylene chloride (1.2 mL), and the mixture was stirred for 50 min. Separately, to a solution of 4d (150 mg, 0.176 mmol) in dimethylformamide (4.0 mL) was added Pd/C catalyst (10%, 52 mg), and the mixture was hydrogenated in a Parr bomb apparatus (325 psi of H$_2$) for 3 h. The catalyst was removed by filtration through Celite, and the filtrate was immediately added to the activated acid and stirred 2.5 h. Methanol (1.0 mL) was added, the mixture was filtered through Celite, and the filtrate was concentrated *in vacuo*. Flash column chromatography of the residue (1% ammonium hydroxide in methanol) provided the hairpin pepide 2-ImN-Ava-P3.

Data for 1a: yield 85% (81 mg); ^{1}H NMR (CD$_3$OD) δ 7.29 (d, 1 H, *J* = 1.9 Hz), 7.23 (d, 1 H, *J* = 1.1 Hz), 7.21 (d, 1 H, *J* = 1.9 Hz), 7.17 (d, 1 H, *J* = 1.9 Hz), 7.16 (d, 1 H, *J* = 1.9 Hz), 7.12 (d, 1 H, *J* = 1.9 Hz), 7.04 (d, 1 H, *J* = 1.1 Hz), 6.93 (d, 1 H, *J* = 1.9 Hz), 6.91 (d, 1 H, *J* = 1.9 Hz), 6.89 (d, 1 H, *J* = 1.9 Hz), 6.87 (d, 1 H, *J* = 1.9 Hz), 6.78 (d, 1 H, *J* = 1.9 Hz), 4.07 (bs, 2 H), 4.04 (s, 3 H), 3.91 (s, 3 H), 3.88 (s, 3 H), 3.86 (s, 6 H), 3.84 (s, 3 H), 3.32 (m, 2 H), 2.43 (t, 2 H, *J* = 7.6 Hz), 2.28 (s, 6 H), 1.77 (m, 2 H); IR (neat) 3334 (s), 2931 (w), 1636 (s), 1577 (m), 1559 (m), 1542 (m), 1466 (m), 1436 (m), 1405 (m), 1311 (s), 1260 (m), 1210 (m), 1026 (w) cm^{-1}; UV (H$_2$O) λ$_{max}$ (ε) 246 (36 600), 304 (42 500) nm; FABMS *m/e* 878.4174 (M + H, 878.4225 calcd for C$_{42}$H$_{52}$N$_{15}$O$_7$).

Data for 1b: yield 78% (80 mg); ^{1}H NMR (DMSO-*d$_6$*) δ 7.38 (d, 1 H, *J* = 0.9 Hz), 7.27 (d, 1 H, *J* = 1.9 Hz), 7.23 (d, 1 H, *J* = 1.9 Hz), 7.19 (d, 1 H, *J* = 1.8 Hz), 7.18 (d, 1 H, *J* = 1.9 Hz), 7.17 (d, 1 H, *J* = 1.8 Hz), 7.14 (d, 1 H, *J* = 1.9 Hz), 7.03 (d, 1 H, *J* = 1.0 Hz), 7.02 (d, 1 H, *J* = 1.8 Hz), 6.87 (d, 1 H, *J* = 1.9 Hz), 6.84 (d, 1 H, *J* = 1.9 Hz), 6.81 (d, 1 H, *J* = 1.8 Hz), 3.98 (s, 3 H), 3.83 (bs, 9 H), 3.80 (s, 3 H), 3.78 (s, 3 H), 3.43 (m, 2 H), 3.17 (t, 2 H, *J* = 6.4 Hz), 2.52 (m, 2 H), 2.22 (t, 2 H, *J* = 7.0 Hz), 2.12 (s, 6 H), 1.59 (m, 2 H); IR (neat) 3338 (m), 2925 (w), 1638 (s), 1585 (s), 1534 (s), 1466 (m), 1438 (s), 1401 (m), 1260 (m), 1206 (m) cm^{-1}; UV (H$_2$O) λ$_{max}$ (ε) 244 (36 100), 306 (48 700) nm; FABMS *m/e* 892.4331 (M + H, 892.4329 calcd for C$_{43}$H$_{54}$N$_{15}$O$_7$).

Data for 1c: yield 55% (13 mg); ^{1}H NMR (CD$_3$OD) δ 7.28 (d, 1 H, *J* = 1.9 Hz), 7.23 (d, 1 H, *J* = 1.1 Hz), 7.15 (d, 3 H, *J* = 1.8 Hz), 7.09 (d, 1 H, *J* = 1.9 Hz), 7.04 (d, 1 H, *J* = 1.1 Hz), 6.90 (d, 1 H, *J* = 1.9 Hz), 6.88 (d, 1 H, *J* = 1.9 Hz), 6.81 (d, 1 H, *J* = 1.9 Hz), 6.80 (d, 1 H, *J* = 1.9 Hz), 6.77 (d, 1 H, *J* = 1.9 Hz), 4.04 (s, 3 H), 3.90 (s, 3 H), 3.87 (s, 3 H), 3.86 (s, 3 H), 3.85 (s, 3 H), 3.84 (s, 3 H), 3.38 (t, 2 H, *J* = 6.3 Hz), 3.30 (m, 2 H), 2.45–2.38 (m, 4 H), 2.28 (s, 6 H), 1.96 (m, 2 H), 1.77 (m, 2 H); IR (neat) 3384 (m), 2936 (w), 1637 (s), 1579 (m), 1542 (m), 1466 (m), 1406 (m), 1261 (m) cm^{-1}; UV (H$_2$O) λ$_{max}$ (ε) 244 (38 900), 308 (48 100) nm; FABMS *m/e* 906.4487 (M + H, 906.4500 calcd for C$_{44}$H$_{56}$N$_{15}$O$_7$).

Data for 1d: yield 72% (116 mg); ^{1}H NMR (DMSO-*d$_6$*) δ 7.38 (d, 1 H, *J* = 0.6 Hz), 7.27 (d, 1 H, *J* = 1.8 Hz), 7.23 (d, 1 H, *J* = 1.9 Hz),

7.19 (bs, 3 H), 7.16 (d, 1 H, $J = 1.9$ Hz), 7.03 (d, 1 H, $J = 0.8$ Hz), 7.01 (d, 1 H, $J = 1.8$ Hz), 6.87 (d, 2 H, $J = 1.7$ Hz), 6.80 (d, 1 H, $J = 1.7$ Hz), 3.98 (s, 3 H), 3.83 (bs, 6 H), 3.81 (s, 3 H), 3.78 (bs, 6 H), 3.43 (m, 2 H), 3.17 (b, 2 H), 2.22 (m, 4 H), 2.12 (s, 6 H), 1.60–1.46 (m, 6 H); IR (neat) 3301 (m), 2935 (w), 1632 (s), 1581 (s), 1535 (s), 1506 (m), 1466 (m), 1432 (m), 1401 (m), 1260 (m), 1204 (m) cm^{-1}; UV (H$_2$O) λ_{max} (ϵ) 246 (38 700), 310 (52 900) nm; FABMS m/e 920.4644 (M + H, 920.4640 calcd for C$_{45}$H$_{58}$N$_{15}$O$_7$).

Construction of Plasmid DNA. Using T4 DNA ligase, the plasmid pMM5 was constructed by ligation of an insert, 5'-TCGACATGA-CATTCGTCCACATTGTTAGACCACGATCGTTTTT-CGCATG-'3 and 5'-CGAAAAACGATCGTGGTCTAACAATGTG-GACGAATGTCATG-3', into pUC19 previously cleaved with *Sal*I and *Sph*I. Ligation products were used to transform Epicurian Coli XL 1 Bluecompetent cells. Colonies were selected for α-complementation on 25 mL Luria-Bertani medium agar plates containing 50 μg/mL ampicillin and treated with XGAL and IPTG solutions. Large-scale plasmid purification was performed using Qiagen purification kits. Plasmid DNA concentration was determined at 260 nm using the relation 1 OD unit = 50 μg/mL duplex DNA. The plasmid was digested with *Eco*RI, labeled at the 3'-end, and digested with *Bsr*BI. The 135 base pair restriction fragment was isolated by nondenaturing gel electrophoresis and used in all experiments described here. Chemical sequencing reactions were performed as described.[12,13] Standard techniques were employed for DNA manipulations.[14]

Quantitative DNase I Footprint Titration. All reactions were executed in a total volume of 40 μL with final concentrations of each species as indicated. The ligands, ranging from 2 μM to 10 pM, were added to solutions of radiolabeled restriction fragment (20 000 cpm), Tris·HCl (10 mM, pH 7.0), KCl (10 mM), MgCl$_2$ (10 mM), and CaCl$_2$ (5 mM) and incubated for 1 h at 22 °C. Footprinting reactions were initiated by the addition of 4 μL of a stock solution of DNase I (0.04 unit/mL) containing 1 mM dithiothreitol and allowed to proceed for 5 min at 22 °C. The reactions were stopped by addition of a 3 M sodium acetate solution containing 50 mM EDTA, and ethanol precipitated. The reactions were resuspended in 100 mM Tris–borate–EDTA/80% formamide loading buffer and electrophoresed on 8% polyacrylamide denaturing gels (5% cross-link, 7 M urea) at 2000 V for 1 h. The footprint titration gels were dried and quantitated using storage phosphor technology.

Apparent first-order binding constants were determined as previously described.[1c,5a] The data were analyzed by performing volume integrations of the 5'-TGTTA-3' and 5'-TGACA-3' target sites and a 5'-AGAG-3' reference site. The apparent DNA target site saturation, θ_{app}, was calculated for each concentration of peptide using the following equation:

(12) Iverson, B. L.; Dervan, P. B. *Nucleic Acids Res.* **1987**, *15*, 7823–7830.
(13) Maxam, A. M.; Gilbert, W. S. *Methods in Enzymology* **1980**, *65*, 499–560.
(14) Sambrook, J.; Fritsch, E. F.; Maniatis, T. *Molecular Cloning*; Cold Spring Harbor Laboratory: Cold Spring Harbor, NY, 1989.

$$\theta_{app} = 1 - \frac{I_{tot}/I_{ref}}{I_{tot}{}^{\circ}/I_{ref}{}^{\circ}} \qquad (1)$$

where I_{tot} and I_{ref} are the integrated volumes of the target and reference sites, respectively, and $I_{tot}{}^{\circ}$ and $I_{ref}{}^{\circ}$ correspond to those values for a DNase I control lane to which no peptide has been added. At higher concentrations of peptide (>2 μM), the reference sites become partially protected, resulting in low θ_{app} values. For this reason, concentrations >2 μM were not used. The ([L]$_{tot}$, θ_{app}) data points were fit to a Langmuir binding isotherm (eq 2, $n = 1$) by minimizing the difference between θ_{app} and θ_{fit}, using the modified Hill equation:

$$\theta_{fit} = \theta_{min} + (\theta_{max} - \theta_{min})\frac{K_a{}^n[L]^n{}_{tot}}{1 + K_a{}^n[L]^n{}_{tot}} \qquad (2)$$

where [L]$_{tot}$ corresponds to the total peptide concentration, K_a corresponds to the apparent monomeric association constant, and θ_{min} and θ_{max} represent the experimentally determined site saturation values when the site is unoccupied or saturated, respectively. Data were fit using a nonlinear least-squares fitting procedure of KaleidaGraph software (version 2.1, Abelbeck software) running on a Macintosh IIfx computer with K_a, θ_{max}, and θ_{min} as the adjustable parameters. The goodness of fit of the binding curve to the data points is evaluated by the correlation coefficient, with $R > 0.97$ as the criterion for an acceptable fit. Three sets of acceptable data were used in determining each association constant. All lanes from each gel were used unless visual inspection revealed a data point to be obviously flawed relative to neighboring points. The data were normalized using the following equation:

$$\theta_{norm} = \frac{\theta_{app} - \theta_{min}}{\theta_{max} = \theta_{min}} \qquad (3)$$

The best fit isotherms for 2-ImN-Gly-P3 binding the 5'-TGTTA-3' and 5'-TGACA-3' sites consistently give worse fits than those for 2-ImN-GABA-P3 binding these sites. Visual inspection of the binding curves for the former peptide reveals that the increase in θ_{max} near half-saturation of the site is steeper than expected from the fitted curve. Fitting of these data to a general Hill model (eq 2) with K_a, θ_{max}, θ_{min}, and n as adjustable parameters afforded best fit values of n greater than 2.0 in all cases. Therefore, the reported binding affinities for 2-ImN-Gly-P3 binding the 5'-TGTTA-3' and 5'-TGACA-3' sites were obtained by performing fits with a modified Hill eqation (eq 2, $n = 2$). The ([L]$_{tot}$, θ_{app}) data points for 2-ImN-GABA-P3 binding these sites were adequately described by Langmuir binding isotherms consistent with a 1:1 peptide–DNA complex (eq 2, $n = 1$). We note explicitly that treatment of the data in this manner does not represent an attempt to model a binding mechanism. Rather, we have chosen to compare values of the apparent first-order dissociation constant, because this parameter represents the concentration of peptide at which the binding site is half-saturated.